

# Revision of photo-current model of terahertz wave generation by two-color femtosecond laser filamentation in air

Jiayu Zhao<sup>1</sup>, Yizhu Zhang<sup>2</sup> and Weiwei Liu<sup>1</sup>

<sup>1</sup> Institute of Modern Optics, Nankai University, Key Laboratory of Optical Information Science and Technology, Ministry of Education, Tianjin 300071, China

<sup>2</sup> Shanghai Advanced Research Institute, Chinese Academy of Sciences, Shanghai 201210, China

**Abstract**—The conventional photo-current model of terahertz wave generation by femtosecond laser filamentation has been improved with taking into account the interaction between the THz pulse and the plasma inside the filament. The results given by this revised model are consistent with the macroscopic four wave mixing mode.

## I. INTRODUCTION

T Hz pulse generated by the femtosecond laser filament in air has received intense research interest recently<sup>1</sup>.

Particularly, because via appropriate optical adjustment, one may locate the filament at a remote distance as far as a few hundred metres, THz remote sensing has been proposed by using this technique to overcome the strong diffraction and the energy attenuation due to water vapour absorption in air<sup>2</sup>.

Two models have been often referred to account for the THz emission during the filamentation<sup>3,4</sup>. A microscopic polarization scheme attributes the THz emission to the free electron drifting current driven by the femtosecond laser field. While, an alternative four-wave mixing (FWM) model based on the perturbation theory<sup>5</sup>. Nevertheless, the intrinsic connection between the microscopic polarization scheme and the macroscopic four-wave mixing model remains mysterious. The current work is devoted to bridging the photocurrent model and the four-wave mixing model. According to our results, an improved photocurrent model which takes into account the propagation effect of the THz pulse during the filamentation would reproduce the major characteristics of the THz pulses generated inside the filament.

## II. RESULTS

By using an electro-optic sampling technique, the instantaneous field vector of the THz pulse generated by mixing a near infrared femtosecond pulse and its second harmonic in air has been investigated. Two orthogonal components of THz transient, namely,  $E_{\text{THz},X}$  and  $E_{\text{THz},Y}$  were detected as a function of the BBO crystal rotation angle  $\theta$  (XYZ is our laboratory coordinate system). By further projecting  $E_{\text{THz},X}$  and  $E_{\text{THz},Y}$  onto the  $o$ ,  $e$  axis,  $E_{\text{THz},o}$  and  $E_{\text{THz},e}$  can be retrieved. The measured  $A_{\text{THz},o}$  and  $A_{\text{THz},e}$  are shown in Fig. 1 as open circles.

While recording THz waveforms by EOS setup, the measurements on the nitrogen ( $N_2$ ) fluorescence signal, which is emitted from the plasma column, have also been performed.  $N_2$  fluorescence signal at 337 nm was selected by an interference filter and collected by a fused silica lens onto a photomultiplier tube (PMT) when  $\theta$  is varied. The strength of the  $N_2$  fluorescence signal, which is a good indication of the free electron density ( $N_e$ )<sup>6</sup>, was recorded as a function of  $\theta$  and depicted in Fig. 2 as blue open circles.

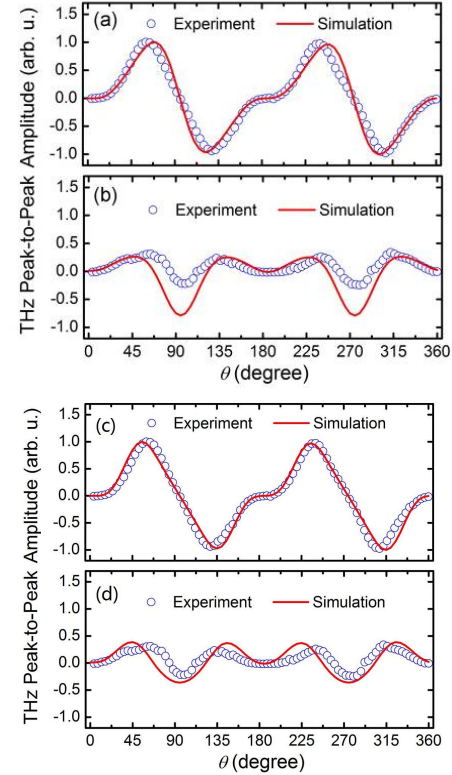


**Fig. 1.** (a)-(b) Simulated  $A_{\text{THz},o}$  and  $A_{\text{THz},e}$  based on the conventional photo-current model as red line, and the experimental results are shown as blue open circles, respectively. (c)-(d) Same as (a) and (b) but taking into account interaction of THz pulse with plasma.

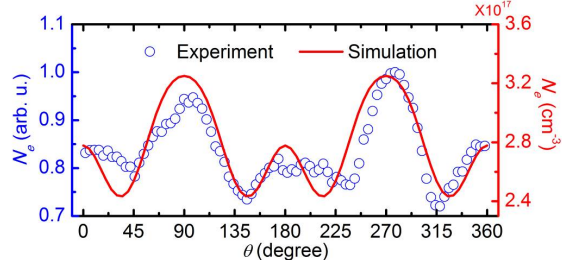


**Fig. 2.**  $N_e$  as a function of  $\theta$ . Blue open circles: experimental measurement; red solid line: simulation prediction

In the following, correlated study of  $N_e$  and  $E_{\text{THz},o}$ ,  $E_{\text{THz},e}$  as a function of  $\theta$  will be carried out, based on the well-known static tunneling ionization model and photocurrent model.

In both the static tunneling ionization model and the photocurrent model describing THz generation through laser-plasma interaction, the knowledge about the temporal evolution of two-color laser field at the focus is essential. Due to the birefringence of BBO crystal and dispersion in air, the laser field distortion during the propagation prior to focus has to be taken into account. The two-color laser field at the focus could be split as the following:

$$\vec{E}(t) = E_o(t)\vec{o} + E_e(t)\vec{e} = E_{1,o}(t)\vec{o} + E_{1,e}(t)\vec{e} + E_{2,e}(t)\vec{e}, \quad (1)$$

where the subscripts 1 and 2 denote the fundamental laser (FL) and its second harmonic (SH), respectively. The subscripts *o* and *e* indicate the polarizations parallel to the ordinary and extraordinary refractive index axes of the BBO crystal, respectively. In the coordinate moving at the group velocity of  $E_{1,o}$ ,  $E_{1,o}$ ,  $E_{1,e}$  and  $E_{2,e}$  could be expressed as:

$$\begin{aligned} E_{1,o}(t) &= E_1 \exp\left(-\frac{t^2}{a^2}\right) \cdot \sin\theta \cdot \cos[\omega t - (n_{1,o} - n_{1,g,o})\frac{\omega}{c}L_1 - (n_{1,a} - n_{1,g,a})\frac{\omega}{c}L_2)] \\ E_{1,e}(t) &= E_1 \exp\left(-\frac{(t-\tau_1)^2}{a^2}\right) \cdot \cos\theta \cdot \cos[\omega(t-\tau_1) - (n_{1,e} - n_{1,g,e})\frac{\omega}{c}L_1 - (n_{1,a} - n_{1,g,a})\frac{\omega}{c}L_2)] \\ E_{2,e}(t) &= \beta E_1^2 \exp\left(-\frac{2(t-\tau_2)^2}{a^2}\right) \sin^2\theta \cdot \cos[\omega_2(t-\tau_2) - (n_{2,e} - n_{2,g,e})\frac{\omega_2}{c}L_1 - (n_{2,a} - n_{2,g,a})\frac{\omega_2}{c}L_2 + \varphi] \end{aligned} \quad (2)$$

where  $E_1$  is the peak amplitude of the fundamental laser field,  $a$  is half the pulse duration of the amplitude envelop at  $1/e$  level, connected to the FWHM of the pulse intensity via  $a = \text{FWHM}/\sqrt{2\ln 2}$ , e.g.  $a = 42.47$  fs when FWHM = 50 fs.  $\beta$  is a proportional factor related to SH conversion efficiency, and  $\varphi$  is the relative phase between FL and SH.  $L_1$  and  $L_2$  denote the thickness of BBO crystal (100  $\mu\text{m}$ ) and the distance from the back surface of BBO to the focus (5 cm).  $\tau_1$  and  $\tau_2$  account for the group delays of  $E_{1,e}$  and  $E_{2,e}$  in BBO crystal ( $L_1$ ) and air ( $L_2$ ) compared with  $E_{1,o}$ .  $\tau_1$  and  $\tau_2$  could be calculated according to the experimental geometry, the refractive indices and group indices in both air and BBO crystal.

The free electron generation dynamic plays a crucial role when dealing with THz generation by femtosecond laser filament in air<sup>3,7</sup>. The ionization rate  $R(t)$  could be commonly described by the static tunneling ionization model following Ref. [1]:

$$R(t) = \frac{a}{A(t)} \exp\left(-\frac{b}{A(t)}\right), \quad (3)$$

where  $A(t) = |\vec{E}(t)|/E_a$  is the electric field in atomic units and

$$\begin{cases} a = 4\omega_a r_H^{5/2} \\ b = (2/3)r_H^{3/2} \\ E_a = \kappa^3 m^2 e^5 / \hbar^4 \approx 5.14 \times 10^{11} \text{ V/m} \\ \omega_a = \kappa^2 m e^4 / \hbar^3 \approx 4.13 \times 10^{16} \text{ s} \end{cases} \quad (4)$$

$\omega_a$  corresponds to the atomic frequency unit,  $r_H = U_{\text{ion}}/U_H$  indicates the ionization potential of the gas molecules under consideration relative to that of hydrogen ( $U_H = 13.6$  eV) and  $\square = (4\pi\epsilon_0)^{-1}$ . In the simulations, the air is considered as being composed of 78 % nitrogen and 22% oxygen with  $U_{\text{ion},N2} = 15.6$  eV and  $U_{\text{ion},O2} = 12.1$  eV. Hence, the electron density  $N_e(t)$  is given by:

$$\begin{cases} dN_e(t) = dN_e(t)_{N_2} + dN_e(t)_{O_2} \\ \int dN_e(t)_{N_2} = R(t)_{N_2} [N_{0,N_2} - N_e(t)_{N_2}] dt \\ \int dN_e(t)_{O_2} = R(t)_{O_2} [N_{0,O_2} - N_e(t)_{O_2}] dt \end{cases} \quad (5)$$

Experimental free electron density distribution with respect to  $\theta$ , namely,  $N_e(\theta)$ , shown in Fig. 2 as blue open circles, can be reproduced by time integral of  $N_e(t)$  in Eq. (5) at a varied  $\theta$ . The simulation results are shown as red line in Fig. 2.

With the free electron density  $N_e(t)$  obtained by Eq. (5), the electron drifting current  $J(t)$  can be computed as

$J(t) = -\int_{-\infty}^{\infty} eN_e(t_0)v(t;t_0)dt_0$ , where  $v(t;t_0)$  denotes the electron velocity under the laser field given by  $v(t;t_0) = -\frac{e}{m} \int_{t_0}^t E(t')dt'$ . The electromagnetic radiation  $E_{EM}(t)$  is determined by  $E_{EM}(t) \propto \partial J(t)/\partial t$  and the radiation spectrum is given by the Fourier transformation of  $E_{EM}(t)$ . The corresponding THz waveform  $E_{\text{THz}}(t)$  emission from the two-color laser field is retrieved from the radiation spectrum by low frequency filtering (< 2 THz in our experimental condition). It is worth mentioned that since  $E(t)$  can be divided into a pair of orthogonal components, i.e.  $E_o(t)$  and  $E_e(t)$  (see Eq. (1)), we actually calculated  $E_{\text{THz},o}(t)$  and  $E_{\text{THz},e}(t)$ , whose polarizations parallel to *o* axis and *e* axis of the BBO crystal, by substituting  $E(t')$  in  $v(t;t_0) = -\frac{e}{m} \int_{t_0}^t E(t')dt'$  with  $E_o(t')$  and  $E_e(t')$ . The simulated  $A_{\text{THz},o}$  and  $A_{\text{THz},e}$  are shown in Fig. 1(a) and (b) as red lines, together with the experimental results. One can see there is an obvious discrepancy between experimental result and simulation prediction in Fig. 1(b), which could instead be interpreted by the FWM model.

Note that it has been demonstrated that the interaction between the THz pulse and the plasma inside the filament also plays important role during the propagation of the THz pulse<sup>8,9</sup>. Hence, **by taking into account the additional loss induced by this process, the conventional photo current model has been revised**. In order to confirm our hypothesis, the effect of the plasma absorption on THz wave generation during filamentation is investigated. When propagating inside plasma, the THz wave amplitude attenuation caused by the plasma absorption is given by:

$$A'_{\text{THz}}(\theta) = A_{\text{THz}}(\theta)e^{-\alpha(\theta)z} = A_{\text{THz}}(\theta)e^{-z/\delta(\theta)}, \quad (6)$$

where  $\alpha$  represents the loss coefficient of THz wave when it propagates. For the convenience, the skin depth  $\delta = 1/\alpha$  is very often adapted to characterize the loss when a monochromatic electromagnetic wave propagates inside a conductor (in our case, it is a plasma). In order to calculate  $\delta(\theta)$ , the simulated on-axis  $N_e(\theta)$  indicated in Fig. 2 as the red line has been used for calculating the complex refractive index of the filament. Then, Eq. (6) was adopted to modulate the simulated  $A_{\text{THz}}(\theta)$  (red lines in Fig. 1(a) and (b)) with the attenuation factor  $e^{-z/\delta(\theta)}$ , which is originated from plasma adsorption. The resulted  $A'_{\text{THz}}(\theta)$  is normalized and indicated in Fig. 1(c) and (d) as the red lines, along with the experimental measurements as the blue open circles. During calculation, the mean value of  $e^{-z/\delta(\theta)}$  is 0.15, in the same order of magnitude as that given by Ref. [9]. The used  $z$  in  $e^{-z/\delta(\theta)}$  is  $\sim 1$  mm, comparable with the propagation distance of THz wave inside plasma filament suggested in Ref. [8]. The revised model clearly gives better interpretation to the experimental results, being consistent with the macroscopic FWM model.

### III. SUMMARY

In summary, in the current work, correlated study of THz wave generation and electron density  $N_e$  has been carried out as a function of BBO crystal rotation angle  $\theta$  during two-color femtosecond laser filamentation in air. We show that the

experimentally recorded THz peak-to-peak amplitudes are much smaller than the simulation outcome mainly at two certain  $\theta$  values. Noting that the maximum  $N_e$  are also located at the same  $\theta$ , the discrepancy between experimental and simulated results could be interpreted by the decrease of the output THz electric field strength during THz wave propagation inside the plasma filament. Two physical processes, namely, plasma absorption and THz wave transmission, have been taken into consideration when performing simulations based on the well-known photocurrent model, and then a better reproduction of the experimental measurement has been achieved.

Based on our results, THz wave generation via two-color femtosecond laser pumping is accompanied by amplitude attenuation induced by plasma absorption and THz wave transmission, simultaneously. In view of this point, an improved photocurrent model which considers the propagation effect of the THz pulse during filamentation would reproduce the characterized polarization states of the generated THz pulse in both orthogonal directions. This improvement has revealed the crucial role of plasma density, established connections between the photocurrent model and the four-wave mixing model, and further provided more choices when one deals with the dynamical process of THz generation and propagation during filamentation in both aspects of microscopic polarization and macroscopic phenomenological analyses.

#### REFERENCES

- [1]. M. D. Thomson, M. Kress, T. Löffler, and H. G. Roskos, “*Broadband THz emission from gas plasmas induced by femtosecond optical pulses: From fundamentals to applications*”, *Laser & Photonics Rev.*, vol. 1, pp. 349-368, 2007.
- [2]. J. Liu, J. Dai, S. L. Chin and X.-C. Zhang, “*Broadband terahertz wave remote sensing using coherent manipulation of fluorescence from asymmetrically ionized gases*”, *Nat. Photonics*, vol. 4 pp. 627-631, 2010.
- [3]. K. Y. Kim, A. J. Taylor, J. H. Glownia, et al. “*Coherent control of terahertz supercontinuum generation in ultrafast laser-gas interactions*”, *Nat. Photonics*, vol. 2, pp. 605-609, 2008.
- [4]. K. Y. Kim, J. H. Glownia, A. J. Taylor, et al. “*Terahertz emission from ultrafast ionizing air in symmetry-broken laser fields*”, *Opt. Express*, vol 15, pp. 4577-4584, 2007.
- [5]. D. J. Cook, R. M. Hochstrasser. “*Intense terahertz pulses by four-wave rectification in air*”, *Opt. Lett.*, vol. 25, pp. 1210-1212, 2000.
- [6]. S. Xu, Y. Zhang, W. Liu, et al. “*Experimental confirmation of high-stability of fluorescence in a femtosecond laser filament in air*”, *Opt. Commun.*, vol 282, pp. 4800-4804, 2009.
- [7]. M. Kress, T. Löffler, S. Eden, et al. “*Terahertz-pulse generation by photoionization of air with laser pulses composed of both fundamental and second-harmonic waves*”. *Opt. Lett.*, vol. 29, pp. 1120-1122, 2004.
- [8]. J. Zhao, W. Chu, L. Guo, et. al., “*Terahertz imaging with sub-wavelength resolution by femtosecond laser filament in air*”, *Sci. Rep.*, vol. 4, pp. 3880, 2014.
- [9]. J. Zhao, Y. Zhang, Z. Wang, et al. “*Propagation of terahertz wave inside femtosecond laser filament in air*”. *Laser Phys. Lett.*, vol. 11, pp. 095302, 2014.